

White-light emissions from p-type porous silicon layers by high-temperature thermal annealing

This content has been downloaded from IOPscience. Please scroll down to see the full text.

2009 EPL 85 27002

(<http://iopscience.iop.org/0295-5075/85/2/27002>)

View [the table of contents for this issue](#), or go to the [journal homepage](#) for more

Download details:

IP Address: 140.113.38.11

This content was downloaded on 25/04/2014 at 13:16

Please note that [terms and conditions apply](#).

White-light emissions from p-type porous silicon layers by high-temperature thermal annealing

W.-C. TSAI¹, J.-C. LIN^{2(a)}, K.-M. HUANG³, P.-Y. YANG⁴ and S.-J. WANG¹

¹ *Institute of Microelectronics, Department of Electrical Engineering, National Cheng Kung University Tainan 70101, Taiwan, ROC*

² *Department of Electronics Engineering, St. John's University - Taipei 25135, Taiwan, ROC*

³ *Institute of Material Science and manufacturing, Chinese Culture University - Taipei 11114, Taiwan, ROC*

⁴ *Department of Electronics Engineering and Institute of Electronics, National Chiao Tung University Hsinchu 300, Taiwan, ROC*

received 6 July 2008; accepted in final form 11 December 2008

published online 26 January 2009

PACS 78.55.Mb – Porous materials

PACS 81.05.Rm – Porous materials; granular materials

PACS 42.70.-a – Optical materials

Abstract – In this study, the white-light emissions, including red, green and blue colors, appearing on the same porous silicon samples are originally introduced by a thermal-annealing method. The SEM, FTIR, and PL are discussed for different annealing temperature cases. The FTIR is used to monitor the chemical bonding structures of the PS samples under different annealing temperatures. The results show that the variation of chemical bonding relates to the variation of the emission wavelength. The emission intensities of the blue-green-light components are enhanced with the increase of annealing temperature. The PL spectra cover the entire visible region under the excitations of He-Cd laser beam, and a strong white-light emission can be observed by the naked eye at room temperature.

Copyright © EPLA, 2009

Introduction. – Porous silicon (PS) structures are widely used to yield efficient visible photoluminescence (PL) at room temperature [1,2]. As we know, white light is very important for optoelectronic devices. However, the visible-light emissions from PS structures usually only appear in the red-light wavelength region by conventional manufacturing methods. The white-light emissions including blue light are still difficult to observe in PS samples to date [3].

Generally, white light is provided by a combination of three light-emitting sources giving red, green and blue (RGB) colors. Therefore, the white-light emission device is usually composed of three color light emission chips [4,5]. Among the RGB colors, the developing of a blue-light emission device is the most difficult. Some researchers are devoted to the methods of blue-shifting from red-light emission [6,7]. In the PS-based light emission, several groups propose the composite methods for white-light emission from red-light-emitting PS structures, such as thermal evaporation [8], and plasma-enhanced chemical vapor deposition (PECVD) [9,10].

In this study, white-light emissions, including RGB colors, are originally obtained by a simple annealing method. By high temperature thermal annealing ($> 500^\circ\text{C}$), the annealed PS samples show strong white PL under ultraviolet (UV) excitation.

To further investigate the structure variations and related optical features after thermal annealing, the scanning electron microscopy apparatus (SEM), Fourier transform infrared spectroscopy (FTIR), and PL are used in our study. In our measurements, the PL spectra (chromophore size) are strongly dependent on the FTIR spectroscopy. This implies that there are strong links between the chemical bonding structures and the PL spectra under high-temperature annealing. In the PL spectra, the scope of the curve contains the entire visible spectrum, and a white-light emission can be clearly observed by the naked eye. Three color bands around 610 nm, 520 nm, and 410 nm are included, which are related to RGB three colors, respectively. Strikingly, the emission intensities of the blue and green light components strongly increase as the annealing temperature increases.

Experiments. – The schematic diagram of the experimental setup for preparing the p-type PS layer is given

^(a)E-mail: jclin@mail.sju.edu.tw

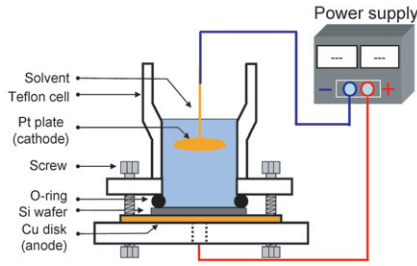
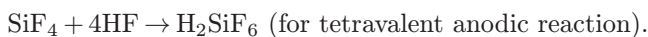
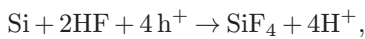
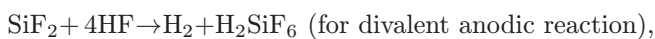
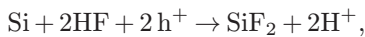


Fig. 1: The schematic diagram of experimental setup for preparing the *p*-type PS layer.

in fig. 1. The main body of the HF electrolyte container is made of Teflon materials. A mixture of HF : C₂H₅OH = 1 : 4 is utilized as the etching solvent here. A copper (Cu) disk is used as the anode, while the cathode is made of platinum (Pt). It should be noted that the apparatus is designed with a vertical arrangement so as to easily remove the hydrogen bubbles from the PS surface and to improve the uniformity of the PS samples. In the present study, the PS samples are prepared on *p*-type Si (100). Prior to the etching process, a sintered aluminum (Al) film is used to form an intimate backside ohmic contact to allow a homogeneous anodization current flow. The anodization etching current is supplied by an external constant current source which is kept at 10 mA/cm². An identical anodic time of 20 min, with anodic current of 10 mA/cm², is used in all cases. To analyze the effect of solution temperature on the anodization process and morphology of the PS films during the etching process, different heating temperature cases are compared in our previous study [11]. At higher-temperature treatment, more electron-hole pairs are generated and the etching effect is enhanced. Increasing the temperature increases the polishing rate and hence decreases the PS film thickness. In order to anodize porous silicon formed under uniform current density, the anodization experiment was done at room temperature. The illustrative equation of the overall process during PS formation can be expressed as below [12,13]:



In the equation, the etching rate is determined by the hole (h⁺) generation.

The PS samples are subsequently subjected to thermal annealing in a quartz tube furnace in argon (Ar) ambient for 60 min. In addition, the top view and cross-section view of PS films are taken using an SEM apparatus (JEOL JSM-6335FNT). The chemical bonding structures of the PS annealed samples are analyzed by FTIR spectroscopy (ASTeX PDS-17 System). Moreover, the PL properties are measured on the PL setup (He-Cd laser and a Hamamatsu R928 photomultiplier detector) at room temperature.

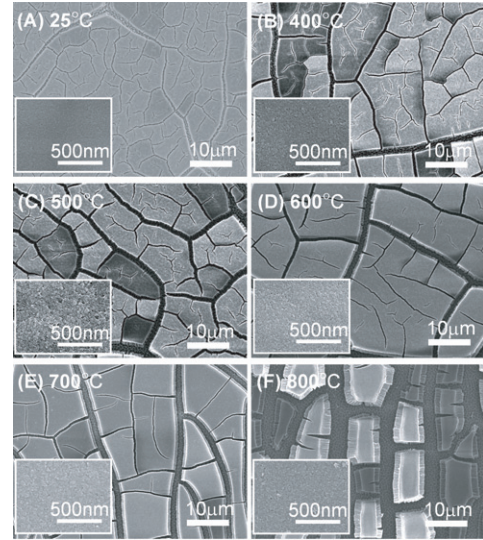


Fig. 2: The top views of SEM images of the PS samples with different annealing temperature: (A) non-annealing case at room temperature, 25 °C, (B) 400 °C, (C) 500 °C, (D) 600 °C, (E) 700 °C, and (F) 800 °C.

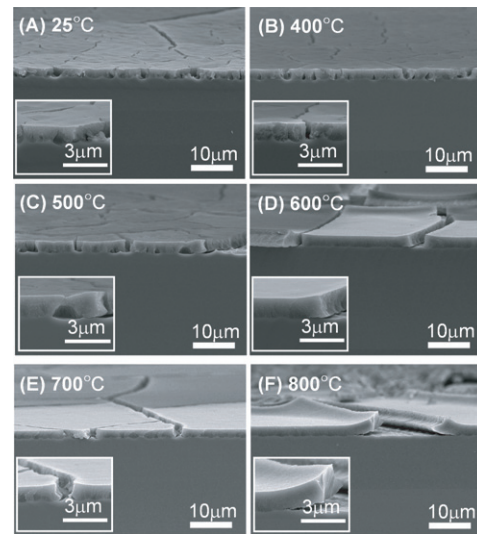


Fig. 3: The cross-section views of SEM images of the PS samples as shown in fig. 2.

Results and discussion. – To analyze the impact of thermal annealing on the *p*-type PS samples and their PL properties, five different annealing temperature cases (ranging from 400 to 800 °C) as well as a non-annealing case are discussed in this paper. They are specified as case A (the non-annealing case at room temperature, 25 °C), case B (400 °C), case C (500 °C), case D (600 °C), case E (700 °C), and case F (800 °C).

In figs. 2 and 3, the top views and cross-section views of SEM images in all cases are shown. It is found that many cracks are formed easily on the sample surfaces as

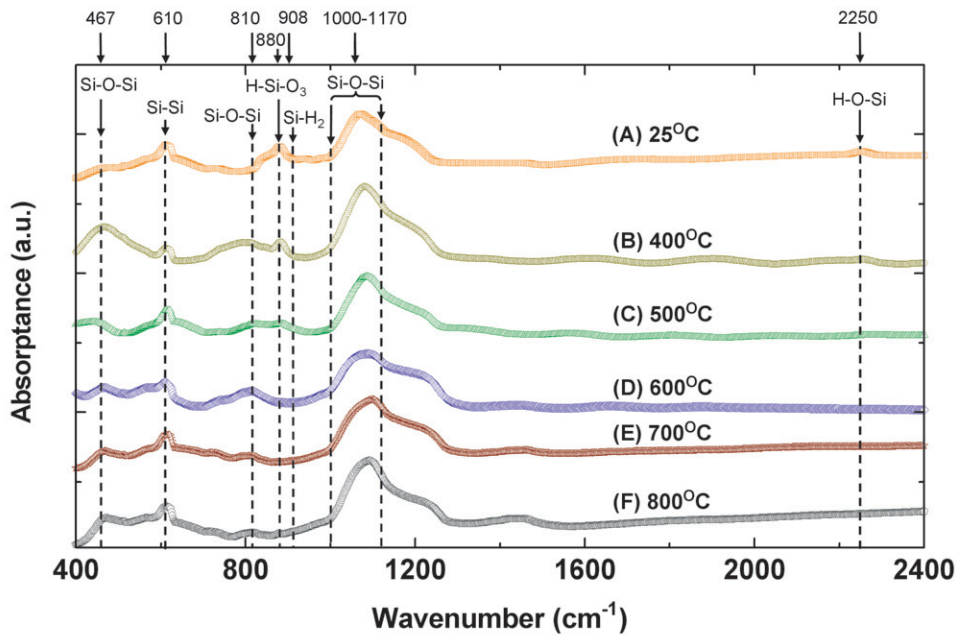


Fig. 4: The FTIR spectroscopy for non-annealed (case A) and post-annealed samples (cases B–F).

the annealing temperature increases, as shown in fig. 2. In addition, the surface membranes curl up easily and deform at higher temperatures, as shown in fig. 3. Both the increase in crack density and curling of PS films at high annealing temperatures are due to the thermal stress. The thermal stress makes matter expand with heat and contract with cold. Because the PS films expand as the temperature increases and contract when they are cooled, many cracks and curling films are formed easily on the PS samples as the annealing temperature increases. The high annealing temperature does not only cause variations in the surface morphology but also causes changes in the chemical bonding structures, especially at temperatures higher than 500 °C.

The FTIR is used to further monitor the chemical bonding structures of the PS samples after different annealing temperatures. Figure 4 shows the FTIR spectroscopy for non-annealed (case A) and post-annealed (cases B–F) samples. As we know, under an annealing process above 500 °C, almost all the hydrogen atoms are removed easily from the surface with enough thermal energy [14,15]. Therefore, it is clear that the H-Si-O₃ bonds (around 880 cm⁻¹), Si-H₂ bonds (908 cm⁻¹), and H-O-Si bonds (around 2250 cm⁻¹) only occur in the cases below 500 °C (case A and case B). In addition, after the annealing treatment, the FTIR peaks around 467 cm⁻¹ and 810 cm⁻¹ originated from the Si-O-Si bonds appear. Also shown in the figure, as the annealing temperature increases, the absorption intensities of the other Si-O-Si bonds (around 1000–1170 cm⁻¹) appearing in all cases also increase. These results indicate that the thermal energy breaks the Si-H bonds and enriches the Si-O-Si bonds (467, 810, and

1000–1170 cm⁻¹). As to the absorption peak at 610 cm⁻¹, it may originate from the Si-Si bonds on the Si substrate.

In this study, a He-Cd laser (325 nm) is used for the measurements on PL properties. Figure 5 shows the PL spectra of PS samples in all cases. In the non-annealing case (case A), an orange-red emission at the 610 nm peak is observed, which is the common result in the previous reported papers [3,16,17]. On the other hand, however, an obvious blue-shifting occurs in all post-annealing cases (case B–F) in this study. Beyond this, the higher annealing temperatures may enhance the emission intensities and broaden the emission spectra when the annealing temperature is increased from 400 °C to 800 °C. (The full widths at half maximums (FWHMs) of the spectra increase from 111 nm to 232 nm.) It indicates that a full-color visible-light emission including red, green and blue colors can be produced in the post-annealing samples.

The left-hand side of fig. 5 shows the naked-eye photos under the excitations of He-Cd laser beam at room temperature. In cases B–F, strong full-color light emissions ranging from 680 to 370 nm are clearly observed. In addition, when the temperature increases, the full-color light emission changes from warm white light to cold white light.

To study the colors constituting the white-light emission during the annealing process, the PL spectra are deconvoluted into three Gaussian peaks at 610, 520 and 410 nm, which correspond to RGB colors, respectively. For further understanding of the correlation between the light emission properties and the chemical bonding structure, the PL spectra and FTIR spectra are examined together. In our experiments on the low-temperature thermal

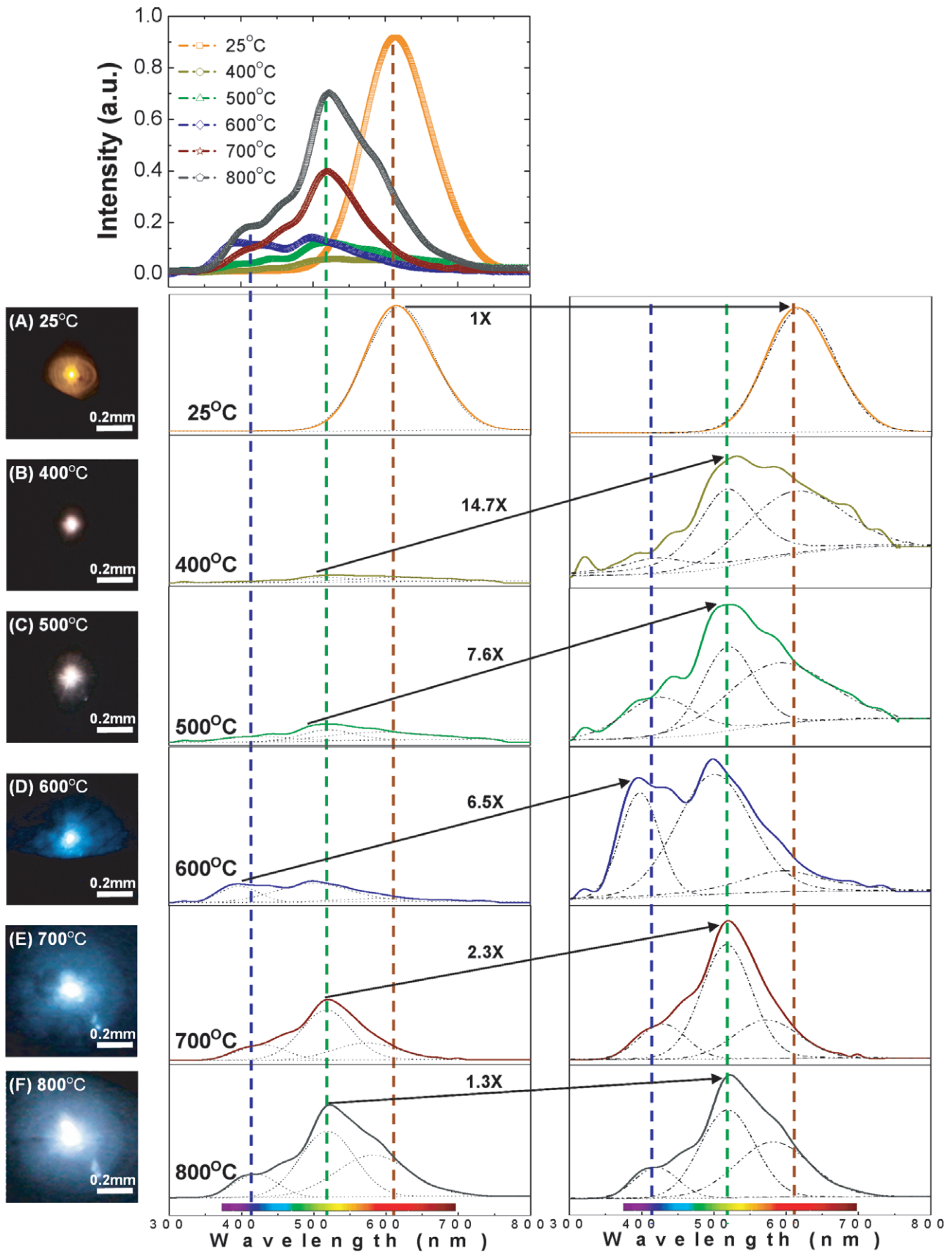


Fig. 5: The PL spectra and the naked-eye photos of cases A–F samples under the excitations of a He–Cd laser beam at room temperature.

annealing cases (25 °C–300 °C), the PL intensity is relatively unchanged below 300 °C, and hence only the 25 °C curve is shown as the representation of low-temperature cases in this paper. Furthermore, the light emission becomes dim obviously at 400 °C. Such results of 25 °C–400 °C are very consistent with the study of Tsai *et al.* [18]. It is believed that the loss of Si-H bonds is the main reason of the drop of the PL intensity from 300 °C to 400 °C. At temperatures up to 400 °C, the peaks at 880 cm⁻¹ (H-Si-O₃, the oxidation of Si-H bond), 908 cm⁻¹ (Si-H₂), and 2250 cm⁻¹ (H-O-Si, the oxidation of Si-H bond) lower down clearly in FTIR spectroscopy (fig. 4). As we know, the red-light emission is strongly related with the Si-H bonds [19]. Therefore, as the temperature rises to 400 °C, the red light component decays with the loss of Si-H bonds.

In this paper, the high-temperature thermal annealing cases (400 °C–800 °C, cases B–F) are focused. When the annealing temperatures are above 400 °C, the light intensity is restored gradually. The recovery of the light intensity at the high-temperature annealing cases can be explained by the oxygen re-passivation of dangling bonds [20] on the Si nanostructures. Even though the continuous decreases (breakings) of Si-H bonds (Si-H₂, H-Si-O₃ and H-O-Si) may reduce the red-light emissions, however, the overall increases of Si-O bonds may cause the light emission to be gradually restored again when the annealing temperature increases from 400 °C to 800 °C. (The area percentage of all Si-O-Si bonds under the FTIR curve may rise from 89.93% to 92.67% when the temperature increases from 400 °C to 800 °C.)

On the other hand, as the Si-H bonds in Si-H₂, H-Si-O₃ and H-O-Si are gradually broken at high temperature, the dangling bonds (*e.g.*, defects (\equiv Si – O)) form. As we know, the dangling bonds may cause green- and blue-light emissions to increase [14]. This is the main reason for the light emission to become stronger when the annealing temperature is higher.

Though the correlation between the chemical bonding and light emission is discussed, however, the PL intensity cannot be predicted precisely only by the chemical bonding situation on the surface. As we know, not only the chemical bonding but also the crystal size would influence the light emission intensity and wavelength. According to the quantum confinement effect [21–23], the shrinking of PS pillar size would cause a blue-shifting, and the more small-enough quantum size pillars would produce the higher intensity of light emission. Therefore, when the annealing temperature increases, the oxidation reactions on Si increases, then the oxygen-passivation layer become thicker and shrink the size of the crystal-Si inside [23,24]. It also would enhance the PL intensity and change the wavelength of light emission. However, this is the reason why the Si-O-Si oscillation in case B (400 °C) is not much lower than the other cases, but it has the lowest PL intensity.

Conclusions. – In conclusion, the clear visible white-light emissions on PS structures are originally obtained by a simple annealing method. By the high-temperature thermal annealing (> 500 °C), the annealed PS samples show strong white PL under UV excitation. When the temperature increases, the full-color light emission changes from warm white light to cold white light. The PL spectra corresponding with the FTIR spectra are examined together for further understanding of the correlation between the chemical bonding structures and the light emission wavelengths as well as intensities. The white-light emissions, including RGB colors, can be observed clearly. The room-temperature white-light emission properties could have a great potential in optoelectronics and microelectronic devices.

This work was supported in part by the National Science Council (NSC) of Taiwan, Republic of China, under Contract No. NSC 96-2221-E-129-012 and No. NSC 96-2221-E-006-285-MY3.

REFERENCES

- [1] MCCORD P., YAU S. L. and BARD A. J., *Science*, **257** (1992) 68.
- [2] CANHAM L. T., *Appl. Phys. Lett.*, **57** (1990) 1046.
- [3] LIN J. C., CHEN W. L. and TSAI W. C., *Opt. Express*, **14** (2006) 9764.
- [4] KIDO J., KIMURA M. and NAGAI K., *Science*, **267** (1995) 1332.
- [5] FUKUDA Y., WATANABE T., WAKIMOTO T., MIYAGUCHI S. and TSUCHIDA M., *Synth. Met.*, **111** (2000) 1.
- [6] HSU J. W. P., TALLANT D. R., SIMPSON R. L., MISSERT N. A. and COPELAND R. G., *Appl. Phys. Lett.*, **88** (2006) 252103.
- [7] ZHAO Y., YANG D., LI D. and JIANG M., *Appl. Surf. Sci.*, **252** (2005) 1065.
- [8] ZHAO X., SCHOENFELD O., KOMURO S., AOYAGI Y. and SUGANO T., *Phys. Rev. B*, **50** (1994) 18654.
- [9] KENYON A. J., TRWOGA P. F. and PITT C. W., *J. Appl. Phys.*, **79** (1996) 9291.
- [10] EDELBERG E., BERGH S., NAONE R., HALL M. and AYDIL E. S., *J. Appl. Phys.*, **81** (1997) 2410.
- [11] TSAI W. C., LIN J. C., CHEN C. W., FU C. H. and WANG S. J., submitted to *Opt. Commun.*
- [12] LEHMANN V. and GIJSELE U., *Appl. Phys. Lett.*, **58** (1991) 856.
- [13] UNAGAMI T., *J. Electrochem. Soc.*, **127** (1980) 476.
- [14] ZHU M., HAN Y., WEHRSPHON R. B., GODET C., ETEMADI R. and BALLUTAUD D., *J. Appl. Phys.*, **83** (1998) 5386.
- [15] OGATA Y. H., YOSHIMI N., YASUDA R., TSUBOI T., SAKKA T. and OTSUKI A., *J. Appl. Phys.*, **90** (2001) 6487.
- [16] LIN J. C., LEE P. W. and TSAI W. C., *Appl. Phys. Lett.*, **89** (2006) 121119.
- [17] LIN J. C., TSAI W. C. and LEE P. W., *Electrochem. Commun.*, **9** (2007) 449.

- [18] TSAI C., LI K.-H., SARATHY J., SHIH S., CAMPBELL J. C., HANCE B. K. and WHITE J. PVL., *Appl. Phys. Lett.*, **59** (1991) 2814.
- [19] TSYBESKOV L., VANDYSHEV JU. V. and FAUCHET P. M., *Phys. Rev. B*, **49** (1994) 7821.
- [20] PETROVA-KOCH V., MUSCHIK T., KUX A., MEYER B. K., KOCH F. and LEHMANN V., *Appl. Phys. Lett.*, **61** (1992) 943.
- [21] CANHAM L. T., *Appl. Phys. Lett.*, **57** (1990) 1046.
- [22] CULLIS A. G. and CANHAM L. T., *Nature*, **353** (1991) 335.
- [23] ZHAO X., SCHOENFELD O., KOMURO S., AOYAGI Y. and SUGANO T., *Phys. Rev. B*, **50** (1994) 18654.
- [24] PROKES S. M., *J. Appl. Phys.*, **73** (1993) 407.